



Comprehensive strategy of conduit guidance combined with VEGF producing Schwann cells accelerates peripheral nerve repair

Ping Wu^{a,1}, Zan Tong^{a,1}, Lihua Luo^{b,1}, Yanan Zhao^a, Feixiang Chen^a, Yinping Li^a, Céline Huselstein^c, Qifa Ye^{d,**}, Qingsong Ye^{b,e,*}, Yun Chen^{a,***}

^a Department of Biomedical Engineering and Hubei Province Key Laboratory of Allergy and Immune Related Diseases, School of Basic Medical Sciences, Wuhan University, Wuhan, 430071, China

^b School and Hospital of Stomatology, Wenzhou Medical University, Wenzhou, Zhejiang, China

^c CNRS UMR 7561 and FR CNRS-INSERM 32.09 Nancy University, Vandœuvre-lès-Nancy, France

^d Zhongnan Hospital of Wuhan University, Institute of Hepatobiliary Diseases of Wuhan University, Transplant Center of Wuhan University, Wuhan, Hubei, 430071, China

^e Center of Regenerative Medicine, Renmin Hospital of Wuhan University, Wuhan, 430060, China

ARTICLE INFO

Keywords:

Angiogenesis
Nerve regeneration
Endogenous secretion
Schwann cells
Vascular endothelial growth factor-A (VEGF-A)

ABSTRACT

Peripheral nerve regeneration requires stepwise and well-organized establishment of microenvironment. Since local delivery of VEGF-A in peripheral nerve repair is expected to promote angiogenesis in the microenvironment and Schwann cells (SCs) play critical role in nerve repair, combination of VEGF and Schwann cells may lead to efficient peripheral nerve regeneration. VEGF-A overexpressing Schwann cells were established and loaded into the inner wall of hydroxyethyl cellulose/soy protein isolate/polyaniline sponge (HSPS) conduits. When HSPS is mechanically distorted, it still has high durability of strain strength, thus, can accommodate unexpected strain of nerve tissues in motion. A 10 mm nerve defect rat model was used to test the repair performance of the HSPS-SC (VEGF) conduits, meanwhile the HSPS, HSPS-SC, HSPS-VEGF conduits and autografts were worked as controls. The immunofluorescent co-staining of GFP/VEGF-A, Ki67 and MBP showed that the VEGF-A overexpressing Schwann cells could promote the proliferation, migration and differentiation of Schwann cells as the VEGF-A was secreted from the VEGF-A overexpressing Schwann cells. The nerve repair performance of the multifunctional and flexible conduits was examined through rat behavioristics, electrophysiology, nerve innervation to gastrocnemius muscle (GM), toluidine blue (TB) staining, transmission electron microscopy (TEM) and NF200/S100 double staining in the regenerated nerve. The results displayed that the effects on the repair of peripheral nerves in HSPS-SC (VEGF) group was the best among the conduits groups and closed to autografts. HSPS-SC (VEGF) group exhibited notably increased CD31⁺ endothelial cells and activation of VEGFR2/ERK signaling pathway in the regenerated nerve tissues, which probably contributed to the improved nerve regeneration. Altogether, the comprehensive strategy including VEGF overexpressing Schwann cells-mediated and HSPS conduit-guided peripheral nerve repair provides a new avenue for nerve tissue engineering.

1. Introduction

Peripheral nervous injuries (PNI) would bring neuropathies to

patients that lead to weakness, paralysis, sensory deprivation, neuropathic pain, and impaired autonomic function [1,2]. Autologous nerve graft transplantation is always the “gold standard” of clinical treatment

Peer review under responsibility of KeAi Communications Co., Ltd.

* Corresponding author. Center of Regenerative Medicine, Renmin Hospital of Wuhan University, 430060, China.

** Corresponding author. Zhongnan Hospital of Wuhan University, Institute of Hepatobiliary Diseases of Wuhan University, Transplant Center of Wuhan University, Wuhan, Hubei, 430071, China.

*** Corresponding author. Department of Biomedical Engineering and Hubei Province Key Laboratory of Allergy and Immune Related Diseases, School of Basic Medical Sciences, Wuhan University, Wuhan, 430071, China.

E-mail addresses: yqf_china@163.com (Q. Ye), qingsongye@hotmail.com (Q. Ye), yunchen@whu.edu.cn (Y. Chen).

¹ Ping Wu, Zan Tong and Lihua Luo contributed equally to this work.

<https://doi.org/10.1016/j.bioactmat.2021.03.020>

Received 18 January 2021; Received in revised form 18 February 2021; Accepted 6 March 2021

2452-199X/© 2021 The Authors. Publishing services by Elsevier B.V. on behalf of KeAi Communications Co. Ltd. This is an open access article under the CC

BY-NC-ND license (<http://creativecommons.org/licenses/by-nc-nd/4.0/>).

in PNI therapy, but it is still restricted by some insurmountable causes, such as donor site morbidity, inadequate donor tissue and deficient functional recovery [3,4]. Nerve guidance conduits (NGCs) are the alternative and promising strategy to guide nerve regeneration [5,6]. NGCs with seed cells and/or cytokines have been investigated to establish favorable microenvironments for nerve regeneration and greatly promote the repairing efficiency [7,8]. For example, human amniotic fluid stem cells (AFSCs) were used to improve the repair of sciatic nerve injury in minipigs [9]. Nerve growth factor (NGF) was immobilized onto the poly (D, L-lactic acid)/chondroitin sulfate/chitosan (PDLLA/CS/CHS) scaffolds to facilitate conduits guided peripheral nerve repair [10]. Although lots of such strategies have been used in neural tissue engineering, the combination still needs to be optimized.

Schwann cells (SCs) are one of most important glial cells in the neural system and generally-used as seed cells in nerve tissue engineering, which could promote axon regeneration [11–13]. Schwann cells were found to blossom into bands of Büngner to facilitate axonal regeneration [14,15]. Engineered Schwann cells in chitosan nerve guides were able to guarantee functional sensory and motor regeneration [16]. In addition, primary Schwann cells from rats were relatively easy to isolate [17]. Therefore, primary Schwann cells were regarded as one of the most promising seed cells in nerve regeneration. Moreover, the nerve repair process is accompanied with angiogenesis, myelination regeneration and axon regeneration [18]. Angiogenesis is particularly important because it initializes the nerve regeneration [19], and vascular endothelial growth factor A (VEGF-A) is the key bio-factor in the process of angiogenesis [20].

Schwann cells could secrete VEGF-A, glial cell trophic factor, neurotrophic factors, and so on. VEGF-A arouses the development and molding of blood vessels and shows potential in protecting motor and sensory neurons. Furthermore, VEGF-A is deemed to protect SCs and trigger themselves' proliferation and migration in an autocrine loop [21]. Meanwhile, if the VEGF-A is not enough at the initial repair stage of nerve injury, it will lead to the failure of Schwann cells mediated nerve repair [18]. Therefore, the appropriate combination of VEGF-A and Schwann cells could prevent the failure of nerve regeneration, effectively reduce the pain of patients and the economic burden of reoperation [22,23].

Adding the SCs to a never guide conduit represents some of the first essential steps in bringing SC-based therapies to the peripheral nerve injuries field [24]. Most importantly, this study represents some of the first essential steps in bringing SC-based therapies to the peripheral nerve injury repair field. Then the combination of Schwann cells and aerobic exercise therapy was proven to enhance the sciatic nerve regeneration [25]. In our previous study, the Schwann cells were combined with pyrroloquinoline quinone to repair the peripheral nerve defect, but there is still a large gap between the result and the effect of autologous transplantation [12]. VEGF-A is a key component of successful blood vessels and nerves regeneration [18]. Transferring VEGF-A genes increases the growth promoting ability of the SCs, particularly in inefficient angiogenesis condition with SCs alone. Lentiviral transfection is good strategy for SCs modulation due to its high integrating capacity, which enables all daughter cells to be labeled with the inserted gene of interest. The lentiviral transfection also allows stable expression of the inserted gene, unlike other viral transfection systems such as adenovirus which may lose its gene expression after cell division. Ex vivo transduction of SCs using lentiviral vectors is straightforward and can give stable and consistent expression over a long period of time *in vivo* [26]. In brief, The VEGF-overexpressing-Schwann cell loaded HSPS showed great clinical potential.

In our previous studies, hydroxyethyl cellulose (HEC)/soy protein isolate (SPI)/polyaniline (PANI) sponges (HSPS) showed good mechanical strength, biocompatibility and could be made into implantable and flexible biosensor [27,28]. This study is committed to assess the peripheral nerve repair capability of HSPS conduits combined with Schwann cells and VEGF-A. Firstly, VEGF-A overexpressing Schwann

cells were established by lentivirus mediated transfection and cells were inoculated and adhered in the inner wall of porous HSPS conduits. Further evaluations of the Schwann cells-mediated and conduit-guided strategy in peripheral nerve injury repair were taken out by *in vivo* analysis, angiogenesis detection and related potential molecular mechanism analysis. This combined strategy may provide a new avenue enhancing angiogenic and regenerative capacity in nerve repair process.

2. Experimental section

2.1. Materials

Hydroxyethyl cellulose powder (viscosity, 30 000 Pa-s) was supplied by Shandong Head Reagent Co. Ltd (Shandong, China). Soy protein isolate (SPI) powder (Mw, 2.05×10^5) was purchased from DuPont Protein Technology (Luohe, China). The aniline monomer (purity 99.98%), epichlorohydrin (ECH), ammonium persulphate (APS), hydrochloric acid (HCl), and acetic acid were from Sinopharm Chemical Reagent Co. Ltd (Shanghai, China). Other chemicals were of analytical grade agents and used without further treatment.

2.2. Fabrication of the HSPS conduits

The hydroxyethyl cellulose/soy protein isolate (HEC/SPI) conduits were fabricated as our recent studies [29,30]. The aniline (0.2 M) was mixed with HCl solution (1 M), and then the faint yellow HEC/SPI conduits with length of 1.2 cm were dipped into the solution and mildly stirred for 30 min in an ice bath. The 100 mL APS solution (0.2 M) was dropped into 100 mL aniline/HCl solution to facilitate the *in situ* polymerization reaction of aniline. According to our previous experimental results, the best *in-situ* polymerization time is 2 h [27]. Then the hydroxyethyl cellulose/soy protein isolate/polyaniline sponge (HSPS) conduits were rinsed with deionized water under stirring more than 48 h for the follow-up research. In addition, this flexibility of prepared HSPS conduit was recorded with camera and the microstructure of HEC/SPI and HSPS conduits were observed with SEM. The mechanical properties of the HEC/SPI and HSPS conduits were detected by the universal testing machine (5943, INSTRON, United States) at a compress rate of 0.5 mm/min. Each conduit with dimensions of length 12 mm, inside diameter 1.8 mm and outside diameter 3.5 mm were used for mechanical property measurement.

2.3. VEGF-A lentivirus construction

In order to construct the VEGF-A overexpression lentivirus plasmid, the SD rat RNA was extracted with Trizol reagent (Invitrogen, USA). The SD rat RNA was reversed into cDNA with the cDNA Reverse Transcription Kit (Bio-Rad, USA). SD rat VEGF-A gene was cloned with PCR, and the primer sequences were as follows: VEGF-A, 5'-CCG GAA TTC CAT GAA CTT TCT GCT CTC TTG G -3' and 5'-CGC GGA TCC GTC ACC GCC TTG GCT TGT CAC-3'; PCR program parameters were 95 °C for 10 min, and then 95 °C for 20 s, 50 °C for 30 s, 72 °C for 60 s and 35 cycles at 95 °C for 20 s, 50 °C for 30 s, 72 °C for 60 s. Amplified fragments were identified and recovered by agarose gel electrophoresis. After the VEGF-A PCR clone product and the lentiviral vectors pCDH-CMV-MCS-EF1-copGFP-T2A-Puro were double-digested with EcoRI and BamHI endonuclease, the T4 ligase was used to insert the double-digested VEGF-A fragments into pCDH-CMV-MCS-EF1-copGFP-T2A-Puro plasmid. Then the recombinant plasmid was transfected into DH-5 α cells. Colony PCR and sequencing verification were used to verified the positive pCDH-CMV-MCS-EF1-copGFP-T2A-Puro-VEGF-A plasmid. The lentiviral packaging vectors (pLP1, pLP2, pLP) and pCDH-CMV-MCS-EF1-copGFP-T2A-Puro/pCDH-CMV-MCS-EF1-copGFP-T2A-Puro-VEGF-A plasmid were co-transfected into 293T cells using Lipofectamine 2000 (Invitrogen, USA). Lentivirus was produced in 293T cells cultured in complete α -MEM at 37 °C and 5% CO₂. After 48 h of transfection, the

lentivirus (control and VEGF-A) was collected by filtering the supernatant of medium through filter with 0.45 μm diameter.

2.4. Schwann cells isolation, lentivirus transfection and conduits fabrication

All animal procedures were done with approval by the Animal Ethical Committee of the Wuhan University (Grant No.: 2018116). The Schwann cells were isolated from the Sprague Dawley (SD) neonatal rats (1–3 days) according to procedures described previously [12]. After the SCs were 90% confluence, they were digested with 0.25% trypsin and seeded onto 6-well plate (1×10^6 cells/well). After 24 h of cell attachment, lentiviruses (control or VEGF-A) were added to the 6-well plates. After 12 h of lentivirus infection, the culture medium was changed to normal complete medium for 24 h, the immunofluorescence and Western blot (WB) detections were used to analyze the expression of VEGF-A protein in Schwann cells.

The sterilized HSPS conduits were put into 6-well plate and 5×10^4 Schwann cells (transfected with control or VEGF-A lentiviruses) suspensions were seeded onto the inner wall of HSPS conduits. And then they were incubated in 37 °C and 5% CO₂ incubator for 24 h before animal experiment.

The Schwann cells on the inner wall of the HSPS conduits were fixed with 4% paraformaldehyde, dehydrated by gradient alcohol and then observed by SEM. The HSPS conduits with Schwann cells (transfected with control lentiviruses) was coded as HSPS-SC, and HSPS conduits with Schwann cells (transfected with VEGF-A lentiviruses) was coded as HSPS-SC(VEGF). The prepared HSPS-SC and HSPS-SC (VEGF) nerve conduits were washed by PBS before the animal experiment in order to avoid the effect of complete medium. Since it was reported conduits filled with laminin-based gel containing 500–700 ng/mL VEGF-A could promote angiogenesis in nerve regeneration [31], HSPS conduits were soaked in the 500 ng/mL VEGF-A protein solution as exogenous VEGF-A coating control conduits. The HSPS nerve guide conduit absorbed VEGF-A protein (P16612, PeproTech, United States) was coded as HSPS-VEGF.

In vitro release profile of VEGF-A from HSPS conduits in each group was evaluated by an enzyme-linked immunosorbent assay (ELISA) method. Briefly, the as-prepared HSPS-VEGF, HSPS-SC and HSPS-SC (VEGF) conduits were immersed in 2 mL complete medium at 37 °C for 7 days. At certain time-points (1, 2, 3, 4, 5, 6 and 7 day), the medium supernatants were collected for ELISA. The VEGF-A concentrations of each group were quantified by VEGF-A ELISA kits (E-EL-R2603c, Elabsience, Wuhan, China) according to manufacturer's instructions.

2.5. Animal experiment

Fifty female SD rats (180–200 g) were fed in the SPF animal house for one week before operation. All SD rats were divided into 5 groups: Autograft, HSPS, HSPS-VEGF, HSPS-SC and HSPS-SC (VEGF). Rats were anesthetized with 1% pentobarbital sodium (30 mg/kg body weight) via intraperitoneal injection (ip). Then the right leg hair was shaven and the leg skin was disinfected. The rat right leg skin was exposed using a scalpel and the muscle tissue was exposed using a blunt dissection. Finally, the sciatic nerve was carefully exposed to the operative horizon. In the autograft group, 10 mm rat sciatic nerve was cut off from the surgical side nerve, and then the nerve was reversed for microscopic suturing. In the other four conduit groups, 12 mm HSPS, HSPS-VEGF, HSPS-SC and HSPS-SC (VEGF) conduits were used and sutured. After the microsurgical suture was completed, the muscle and skin were sutured.

2.6. Western blot analysis

VEGF-A overexpressing Schwann cells and control Schwann cells were collected and total protein extraction kit was used to prepare

protein extract. The regenerated nerve tissues were collected in each group after 3 months of the operation, and tissue protein extraction kit was used for protein extraction. The total proteins were blended with SDS-PAGE loading buffer (Beyotime, China) and then heated at 95 °C for 5 min. Protein samples were loaded on 10% SDS-PAGE and electroplated onto PVDF films (Millipore, USA). The PVDF films were blocked by 5% nonfat milk (Beyotime, China) which was dissolved in TBST (0.15 M NaCl, 0.05% Tween-20, 10 mM Tris-HCl [pH8.0]) for 1 h at 25 °C and subsequently it was incubated overnight at 4 °C with the following primary antibodies: anti-VEGF-A antibody (GB11034, 1:1000 dilution, Servicebio), anti-CD31 antibody (A3181, 1:1000 dilution, Abclonal), anti-VEGFR2 antibody (GB11190, 1:1000 dilution, Servicebio), anti-p-VEGFR2 antibody (AP0392, 1:1000 dilution, Abclonal), anti-ERK antibody (GB11004, 1:1000 dilution, Servicebio), anti-p-ERK antibody (GB11560, 1:1000 dilution, Servicebio), and anti- β -actin antibody (GB1101, 1:2000 dilution, Servicebio). After incubating the films with horseradish peroxidase (HRP)-labeled secondary antibodies (GB23303, 1:3000 dilution, Servicebio) for 60 min, the WB signals were detected by an enhanced chemiluminescence (ECL Western Blotting Substrate, Pierce, USA) system. Density values were determined with the software Image J, and the target genes were normalized to β -actin or total proteins.

2.7. Behavioral analysis

Walking track analysis was performed at three months after the surgery before the animals were killed as reported work [32,33]. The posterior limb footprints of the rats on the track were recorded with red inkpad on the blank sheet of paper. The rat red footprints were obtained and the sciatic function index (SFI) was analyzed with the following equation from previous studies:

$$\text{SFI} = -38.3 \frac{\text{EPL} - \text{NPL}}{\text{NPL}} + 109.5 \frac{\text{ETS} - \text{NTS}}{\text{NTS}} + 13.3 \frac{\text{EIT} - \text{NIT}}{\text{NIT}} - 8.8 \quad (1)$$

Where the PL implies the print length, it was the length of the rat third toe to the heel. TS indicates the toe spread, it was the length of first and the fifth toe. IT represents the length of the second to the fourth toe. The “N” in NPL, NTS and NIT represents the non-operated posterior limb. The “E” in EPL, ETS and EIT represents the experimental posterior limb.

2.8. Electrophysiology examination

The rat sciatic nerve on the operated side was re-opened to conduct the electrophysiology detection under anesthesia at 3 months after operation. The electrophysiology system (RM6240, China) was used to record the myoelectric activity. The 10 mV electrical stimulation was applied to stimulate the action potential of the gastrocnemius muscle at the proximal ends of the injured nerve. The compound muscle action potentials (CMAPs) were recorded and analyzed.

2.9. Gastrocnemius muscles evaluation

Three months after the operation, the gastrocnemius muscles of operated and normal hind limbs were harvested. The wet weight was recorded to muscle weight recovery rate according to equation (2)

$$\text{Wr} (\%) = [\text{Ws} / \text{Wn}] \times 100 \quad (2)$$

Where the Wr represents the muscle weight recovery rate, the Ws indicates the muscle weight of gastrocnemius on the operative side, the Wn is the muscle weight of normal lateral gastrocnemius muscle.

After the gastrocnemius tissues were weighed and photographed, they were cut into halves and fixed into 4% paraformaldehyde solution over 1 day subsequently. After the gastrocnemius muscles were paraffin embedded and sectioned, 6 μm sections were prepared and then

subjected to Masson's trichrome staining. More than 3 fields of the sections were collected for data analysis. The percentage of collagen fiber area was calculated according to equation (3):

$$c (\%) = [b/(a + b)] \times 100 \quad (3)$$

Where the "a" represents the cross-sectional area of muscle fibers, the "b" represents the collagen fiber area, the "c" represents the percentage of collagen fibers.

2.10. Myelination examination

The regenerated nerve was removed along with the conduits 3 months after operation. The regenerated nerve was washed with normal saline, then fixed with 2.5% glutaraldehyde over 1 day at 4 °C. The HSPS conduits were peeled and sliced into 1 μm sections for toluidine blue staining and 50 nm sections for transmission electron microscope (TEM) observation. The density of regenerated nerve fibers was calculated with IPP 6.0 software. The ultrastructures of regenerated nerve were observed by TEM (HT7700, Hitachi, Japan). and TEM images were also analyzed by IPP 6.0 software to calculate the axon diameter and myelin sheath thickness.

2.11. Histological assessment of regenerated nerves

At 3 months of the postoperative feeding, the regenerated nerve tissues in rats were taken out together with the nerve conduits. A portion of regenerated nerve tissues were fixed in 4% paraformaldehyde solution at 4 °C for 24 h. The regenerated nerves were dehydrated, paraffin-embedded and sectioned into 5 μm sections. Then H&E staining was performed and photographed under optical microscope (BX71, OLYMPUS, Japan).

Another portion of the regenerated nerve tissues from rats were fixed with 4% paraformaldehyde, paraffin-embedded to prepare the cryostat sections. In brief, the cryostat sections of the harvested nerve tissues were blocked with 5% goat serum in PBS solution for 1 h at 25 °C. Then, the sections were incubated with anti-CD31 antibody (A3181, 1:1000 dilution, Abclonal) in 4 °C refrigerator for 12 h. After washing with normal saline, the nerve sections were further incubated with secondary antibody (G1215-3, Servicebio) for 1 h. Subsequently, the nerve sections were stained with diaminobenzene for visualization. Cell nuclei were counterstained with hematoxylin. Finally, the immunostained samples were observed using an inverted microscope.

For immunofluorescence staining of regenerated nerves, the paraffin sections were deparaffinized, antigen retrieval blocked and incubated with anti-GFP/VEGF-A (AE012, Abclonal/A0280, Abclonal), anti-GFP/CD68 (AE012, Abclonal/76437, Cell signal), anti-GFP/Ki67 (AE012, Abclonal/12075, Cell signal), anti-GFP/MBP (AE012, Abclonal/78896, Cell signal), anti-NF200/S100 (N4142, Sigma-Aldrich; ab7852, Abcam) or anti-CD34/α-SMA primary antibody (ab81289, Abcam; ab5694, Abcam) at 4 °C for 1 night. And then the sections were incubated with horseradish peroxidase-labeled secondary antibodies (Servicebio, China) for 1 h. The cell nuclei were stained with DAPI dye. Finally, the images were collected with fluorescence microscope (BX51, OLYMPUS, Japan). IPP 6.0 software was used to measure the percentage of positive NF200/S100 staining and regenerated nerve neovascularization density.

2.12. Statistical analysis

All results are presented as mean ± S.E.M. One-way ANOVA followed by post-hoc test was used to compare the means of more than two samples. *P* values of less than 0.05 were considered to be statistically significant.

3. Results

3.1. Preparation of HSPS conduits

Since the conductive matrix is required for nerve impulse conduction, conductive HSPS conduits were fabricated by *in-situ* polymerization of aniline as our recent report [27,28]. As the addition of polyaniline, the biodegradable HEC/SPI conduit changed from primrose yellow to black (Fig. 1A). In addition, Fig. 1B showed that the HSPS conduits can withstand multiple compressions and folds (bending at 180°), which is sufficient to reflect its high flexibility. From the perspective of microstructure, the conduits showed the porous structure (Fig. 1C), which is convenient for the exchange of nutrients between the nerves in the conduit and the outside microenvironment. In the enlarged images of Fig. 1C, we can see that fine particles were appeared in the HSPS conduit as the addition of polyaniline. Besides, the mechanical strength of HSPS conduits was also conducted as shown in Fig. 1D and E. The mechanical strength of HSPS conduits were greatly improved by the *in-situ* polymerization of polyaniline in the HEC/SPI conduits.

3.2. Establish of VEGF-A overexpressing HSPS conduits

In order to construct the HSPS conduits combining VEGF-A, VEGF-A expression lentiviral plasmid was cloned and verified by colony PCR (Fig. A1) and sequencing. Immunofluorescence images of VEGF-A in Schwann cells transfected with control and VEGF-A expression lentivirus were illustrated in Fig. 2A. VEGF-A expression levels were significantly higher in the VEGF-A overexpressing group than in the control group. To quantify VEGF-A protein levels in Schwann cells, Western blot analysis was shown in Fig. 2B. The VEGF-A proteins in VEGF-A overexpressing SCs is significantly higher than that of control SCs, suggesting that Schwann cells overexpressing VEGF-A was successfully established.

SEM images of Schwann cells inoculated and adhered in the inner wall of the HSPS conduits are shown in Fig. 2C. Both VEGF-A overexpressing and control Schwann cells could grow and adhere well to the HSPS conduit inner walls in enlarged SEM images in Fig. 2C. As the expression levels of VEGF-A by different Schwann cells in the HSPS-SC and HSPS-SC(VEGF) conduits would affect the nerve regeneration, ELISA analysis was conducted to detect the accumulated secretion of VEGF-A *in vitro* from HSPS-VEGF, HSPS-SC and HSPS-SC(VEGF) conduits (Fig. 2D). On the day 1, the HSPS-VEGF conduit secreted most of the VEGF-A adsorbed in the HSPS conduits. From the day 2, the release of the VEGF-A in the HSPS-VEGF group conduits was basically over. In contrast, in the HSPS-SC and HSPS-SC(VEGF) groups, VEGF-A was released in a slowly release process, and the secretion of VEGF-A in HSPS-SC(VEGF) conduit was significantly higher than that of HSPS-SC group.

3.3. The Schwann cells behaviors after transplantation in vivo

According to the immunofluorescence co-staining of GFP and VEGF-A in Fig. 3, abundant VEGF-A could be detected both intracellularly and extracellularly in HSPS-SC(VEGF) group, while few VEGF-A positive cells were observed in HSPS-SC control group. Ki67 is a biomarker of cell proliferation, the cell proliferation of Schwann cells after transplantation can be determined by immunofluorescence co-staining of GFP and Ki67. As shown in Fig. A2, the percentage of Ki67⁺/GFP⁺ labeled cells in HSPS-SC(VEGF) group was higher than that of HSPS-SC group. Therefore, the overexpression of VEGF-A in Schwann cells could promote the proliferation of Schwann cells. MBP protein is a myelination differentiation biomarker of Schwann cells, the percentage of MBP⁺/GFP⁺ labeled Schwann cells in HSPS-SC(VEGF) group far outperformed the HSPS-SC group (Fig. A3). It can be seen that the overexpression of VEGF-A in Schwann cells can promote the myelination differentiation of Schwann cells.

In addition, immune response is a really critical issue and we will

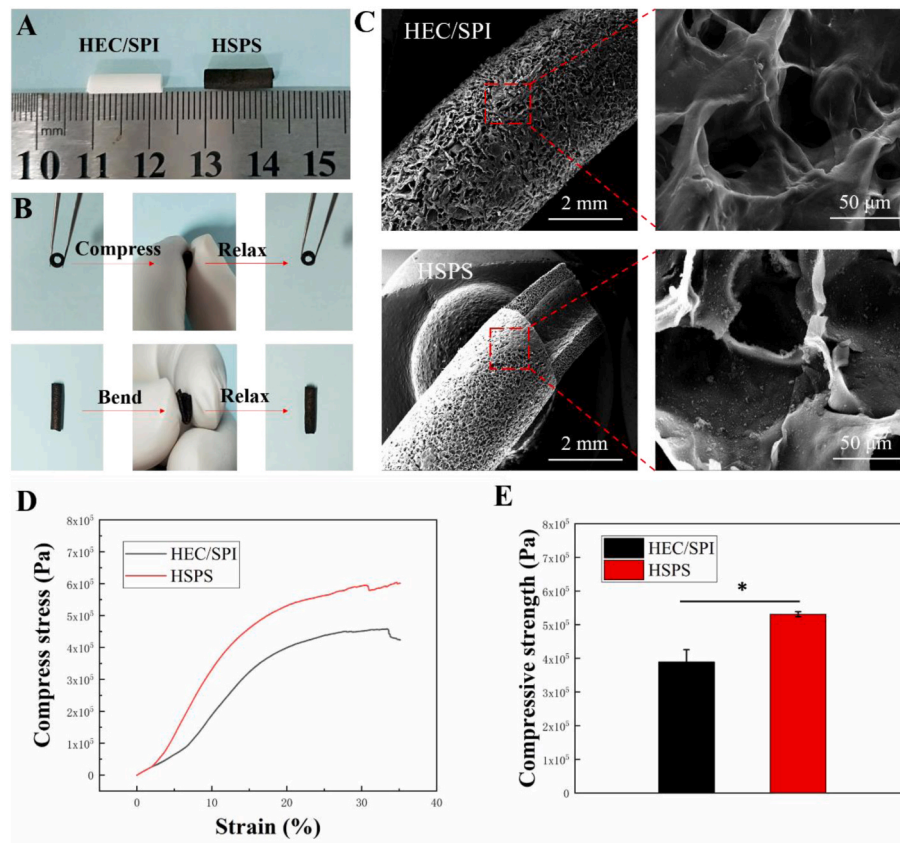


Fig. 1. Preparation of HSPS nerve conduits. (A) The images of HEC/SPI and HSPS conduits; (B) The flexibility of the HSPS conduit; (C) The SEM images of HEC/SPI and HSPS conduits; (D) The compressive stress–strain curves of the HEC/SPI and HSPS conduits; (E) The compressive strength of the HEC/SPI and HSPS conduits, $n = 4$, *: $P < 0.05$.

focus on the immune response during the conduit guided and Schwann cells mediated nerve repair in the future study. According to the immunofluorescence co-staining of GFP and CD68 in [Supplementary Fig. A4](#), no CD68⁺ labeled macrophages were detectable, suggesting hardly any immune response could be detected at 3 months after HSPS-SC(VEGF) conduits transplantation *in vivo*.

3.4. Neurologic function recovery

In order to determine the proper strategy of nerve repair, four conduit groups, HSPS, HSPS-VEGF, HSPS-SC and HSPS-SC (VEGF) conduits were applied to bridge 10 mm sciatic nerve defect with autograft as control. Three months after surgery, the motor functional recovery was assessed in all groups. The rat walking footprints on the surgical side in the Autograft, HSPS, HSPS-VEGF, HSPS-SC and HSPS-SC (VEGF) groups are shown in [Fig. 4A](#), and the footprints of each group were different. According to the information of these footprints and equation (1) in experiment section, we can calculate the SFI values to evaluate the recovery of movement function. The SFI values in autograft, HSPS, HSPS-VEGF, HSPS-SC and HSPS-SC (VEGF) groups were -49.9 , -59.7 , -58.12 , -54.9 and -50.1 , respectively ([Fig. 4B](#)). The SFI value of HSPS-SC(VEGF) was similar to that of autograft, while SFI values of HSPS and HSPS-VEGF were significantly lower than that of autograft. Since the SFI values of the HSPS-SC and HSPS-SC (VEGF) were significantly higher than those of the two other nerve guide conduit groups, indicating that Schwann cells themselves could elevate the SFI index.

The CMAPs tests were further used to detect neurological recovery after 3 months of surgery. [Fig. 4A](#) was representational CMAPs records of the operative limb of the five experimental groups and different

CMAPs signals were detected in the different experimental groups. As demonstrated in [Fig. 4C](#), the mean peak amplitude of CMAPs of autograft, HSPS, HSPS-VEGF, HSPS-SC and HSPS-SC (VEGF) groups are 20.2, 10.4, 11.1, 13.6 and 17.7 mV, respectively. Autograft group had the highest mean peak amplitudes of CMAPs among the five experimental groups. At the same time, there was no significant difference of mean peak amplitudes of CMAPs between the HSPS and the HSPS-VEGF group, suggesting that the VEGF-A adsorbed in the HSPS conduit didn't accelerate the recovery of electrophysiological functions. In [Fig. 4D](#), the mean conduction velocity of CMAPs in Autograft, HSPS, HSPS-VEGF, HSPS-SC and HSPS-SC (VEGF) exhibited 12.56, 6.72, 7.8, 9.7 and 11.8 m/s, respectively. The mean conduction velocity of CMAPs of autograft and HSPS-SC (VEGF) were higher than those of other three conduit groups, while the mean conduction velocity of CMAPs in HSPS-SC was higher than that of non-SCs groups. According to [Fig. 4E](#), the mean latencies of CMAPs in Autograft, HSPS, HSPS-VEGF, HSPS-SC and HSPS-SC(VEGF) groups were 6.4, 10.2, 9.5, 7.7 and 6.5 ms, respectively. The longer the latencies of the CMAPs, the worse the recovery effect of electrophysiology. The experimental results of the latencies were completely contrary to those of the conduction velocity.

These results demonstrated that the electrical signals conduction function of the HSPS-SC(VEGF) group was higher than that in the other three conduit groups, while justly the mean peak amplitude of CMAPs was slightly lower than that of the autograft group. In a word, nerve repair ability of HSPS conduit combined with Schwann cells and endogenous VEGF showed better efficiency in electrophysiological experiment results.

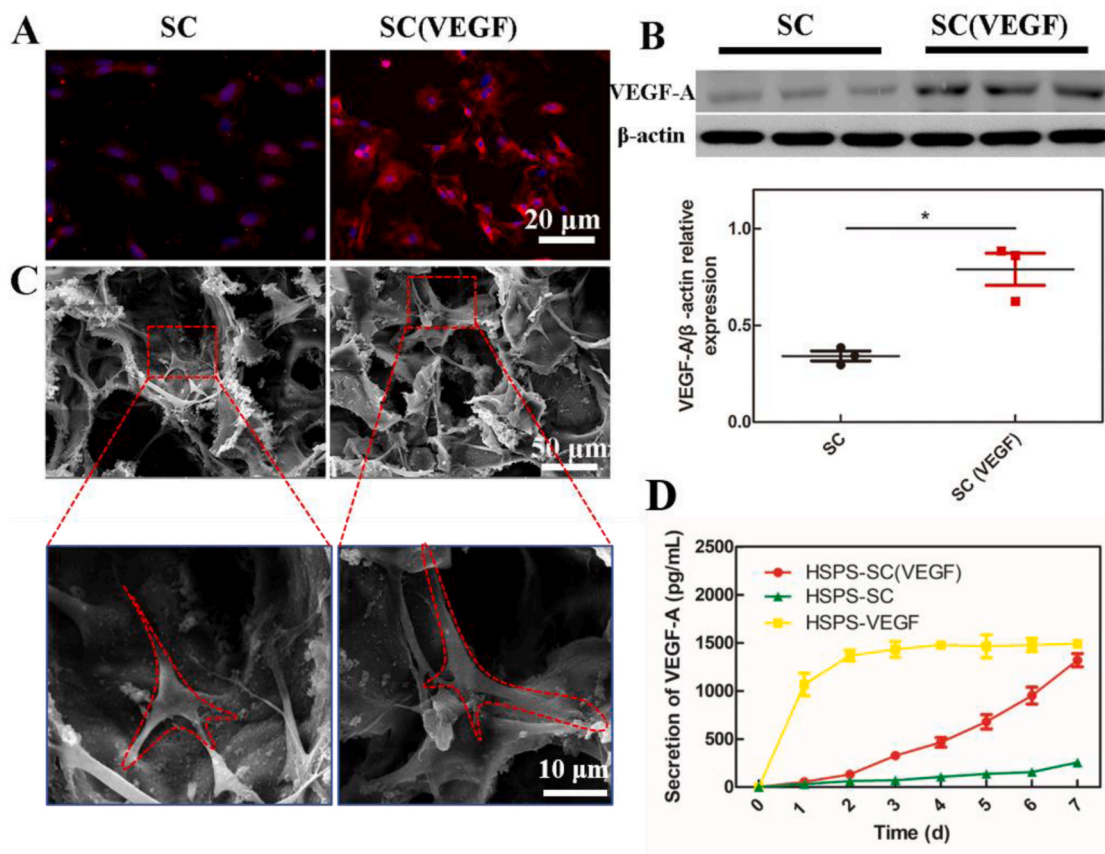


Fig. 2. Establishment of VEGF-A overexpressing conduits. (A) Immunofluorescent co-staining of VEGF-A in Schwann cells and VEGF-A overexpressing Schwann cells, red = VEGF-A, blue = DAPI, scale bar = 20 μm; (B) Western Blot analysis of VEGF-A proteins in Schwann cells and VEGF-A overexpressing Schwann cells, n = 3, *, P < 0.05, the bottom row is the quantification of VEGF-A relative expression levels; (C) SEM images of Schwann cells and VEGF-A overexpressing Schwann cells cultured within inner wall of HSPS nerve guide conduits, the enlarged SEM image shows the morphologies of Schwann cells in the HSPS-SC and HSP-SC(VEGF) groups, the enlarged Schwann cells were labeled with red dotted line; (D) The *in vitro* cumulative release of VEGF-A in HSPS-VEGF, HSPS-SC and HSPS-SC (VEGF) conduits at 1, 2, 3, 4, 5, 6 and 7 days, n = 3.

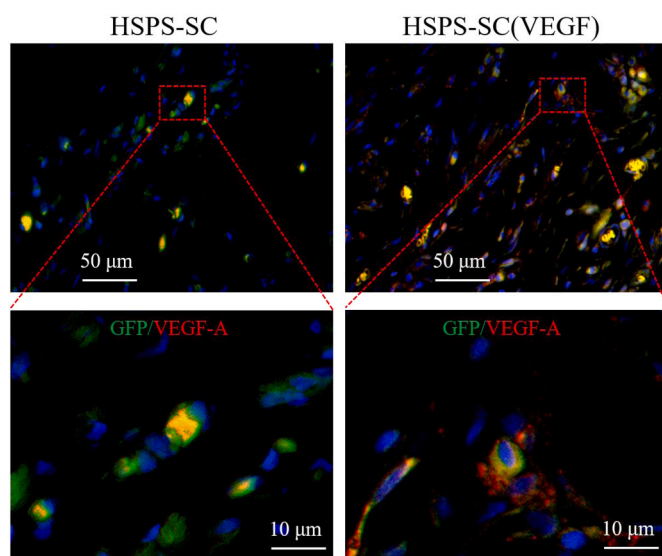


Fig. 3. Immunofluorescent co-staining of GFP and VEGF-A *in vivo*, green = GFP, red = VEGF-A, blue = DAPI.

3.5. Analysis of the gastrocnemius muscle

To analyze the effect of regenerated nerve on gastrocnemius muscle (GM) innervation, the GM of both posterior limbs were harvested. The atrophy degree of the GM in the five groups were recorded with the camera (Fig. 5A). GM were further stained with Masson's dye and the cross-sectional areas of muscle fibers and the collagen fibers were observed and analyzed (Fig. 5B). The GM of the right posterior limb were all smaller than that of left posterior limb in all groups. According to Fig. 5C, the muscle weight recovery rates in the Autograft and HSPS-SC (VEGF) groups showed no significant difference, while the GM muscle weight recovery rates of the HSPS, HSPS-VEGF, HSPS-SC groups were lower than those of autograft and HSPS-SC (VEGF) groups. The GM muscle fiber cross-sectional area and collagen fiber area percentage in the five experiment groups were analyzed in Fig. 5D and E, respectively. Comparing to the autograft group, the muscle fiber cross-sectional areas in HSPS, HSPS-VEGF and HSPS-SC groups were smaller, on the contrary, the collagen fiber area percentages in those groups were significantly larger. Meanwhile, there was no significant difference in muscle fiber cross-sectional area and collagen fiber area percentage between Autograft group and HSPS-SC (VEGF) group.

These data showed that the GM re-innervation capacity in the HSPS-SC (VEGF) group was the best among the four conduit groups, and the degree of re-innervation of the GM was similar to that in autograft.

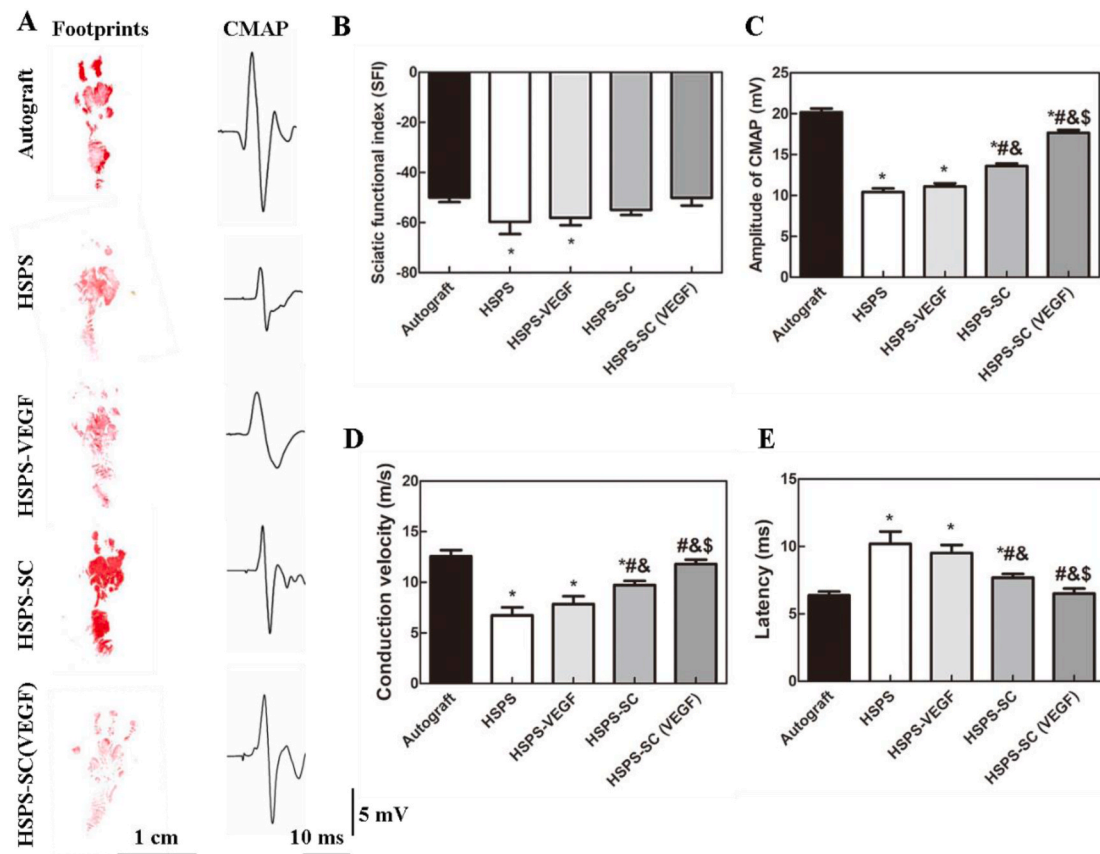


Fig. 4. Neurologic function recovery analysis. (A) Representative images of walking track footprints and representative CMAPs recorded on the repaired nerve; (B) Analysis of SFI values, peak amplitude of CMAPs (C), conduction velocity (D) and latency (E), n = 5, *: P < 0.05, compared with Autograft; #: P < 0.05, compared with the HSPS group; &: P < 0.05, compared with the HSPS-VEGF group; \$: P < 0.05, compared with the HSPS-SC group.

3.6. Regenerated myelin analysis

Regenerated nerves were sectioned and further investigated to compare the repairing capacity of four different conduits and autogenous graft. The toluidine blue (TB) staining images are demonstrated in Fig. 6A. All groups exhibited myelinated nerve fibers. The mean density of myelinated nerve fibers of autograft group, HSPS group, HSPS-VEGF group, HSPS-SC group and HSPS-SC (VEGF) group were 15667.6, 9643.75, 9232.36, 12567.9 and 14610.3 number/mm², respectively (Fig. 6B). The myelination of regenerated nerve fibers of the HSPS-SC (VEGF) was the highest one among the conduit groups, indicating Schwann cells overexpressed VEGF-A could efficiently improve the myelination of regenerated nerve fibers. Notably, HSPS-SC (VEGF) group had similar number of myelinated nerve fibers comparing to autograft group. On the other hand, the density of myelinated nerve fibers in HSPS-SC group was significantly higher comparing to the HSPS and HSPS-VEGF groups, demonstrating that Schwann cells could promote the myelination of regenerated nerve fibers to some certain extent.

TEM images of distal segments from regenerated nerve in the five experiment groups were demonstrated in Fig. 6A. The axon diameter (AD) of HSPS-SC (VEGF) was similar to the AD of autografts, while the AD of HSPS, HSPS-VEGF and HSPS-SC groups were significantly lower than that of autograft. The AD of the HSPS-SC group was larger than that of the HSPS and HSPS-VEGF groups, while there was no difference between HSPS and HSPS-VEGF groups (Fig. 6C). Moreover, the trend of thicknesses of myelin sheaths was consistent with the trend of axon diameters among groups (Fig. 6D). The G-ratio of the myelin sheath represents the ratio of inner diameter to outer diameter. As shown in Fig. 6E, the G-ratio of HSPS-SC (VEGF) group was lowest in the conduit groups, and the HSPS-SC(VEGF) group and autograft group didn't show

any differences. The G-ratio of other three conduit groups were all higher than that of the Autograft group, while there was no difference among the HSPS, HSPS-VEGF and HSPS-SC groups. These data implied that Schwann cells and overexpressed VEGF-A could efficiently promote the myelination of regenerated nerve fibers.

3.7. Immunofluorescence staining analysis

NF200 and S100 were detected to study the remediation efficiency of regenerated nerve. The distal part of regenerated nerves was harvested for immunofluorescence staining as shown in Fig. 7A. NF200 is the specific biomarker for neurofilament and S100 is the biomarker for myelin glial cells. Both NF200 and S100 could be detected in the regenerated nerves in the five groups. The mean percentages of NF200/S100 positive staining of autograft and HSPS-SC(VEGF) were higher than that of HSPS, HSPS-VEGF and HSPS-SC, while the mean percentage of NF200/S100 positive staining in the HSPS-SC was higher than that of HSPS and HSPS-VEGF (Fig. 7B and C).

All in all, the NF200 and S100 immunofluorescence data suggested that the nerve remediation efficiency of HSPS-SC(VEGF) group was the highest one in the conduit groups. The combination of Schwann cells and endogenous VEGF could effectively promote NF200 and S100 expression. Thus, this synergistic strategy promoted the neurofilament and myelin regeneration.

3.8. Effect of Schwann cells overexpressed VEGF-A on angiogenesis

To evaluate angiogenesis in each group, histological and immunohistochemical studies were performed. H&E sections of the regenerated nerve showed that more blood vessels and cells could be observed in the

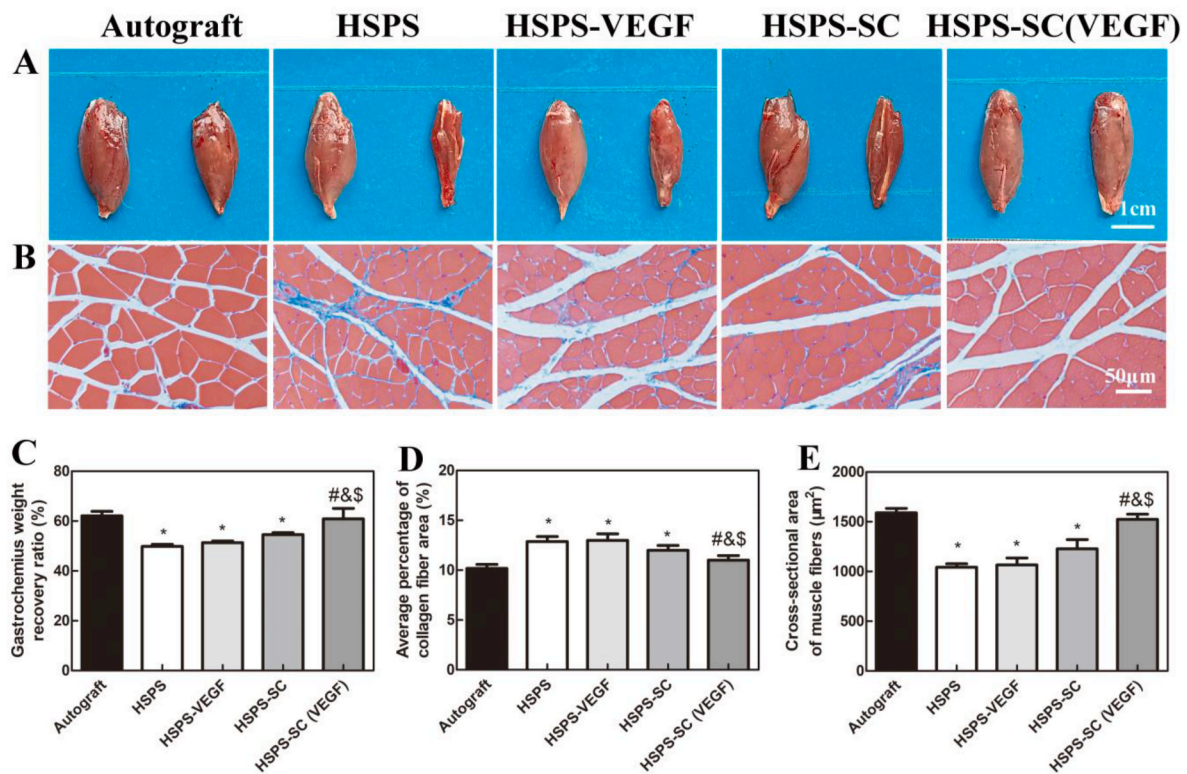


Fig. 5. Histological assessment of gastrocnemius muscles. (A) Images of gastrocnemius muscle between normal side and operative side; (B) Masson's trichrome staining of cross sections of gastrocnemius muscle; (C) The statistical results of the gastrocnemius weight recovery ratio; (D) The statistical results of the cross section area of muscle fibers; (E) The statistical results of the average percentage of collagen fiber area, $n = 5$, *: $P < 0.05$, compared with the Autograft group; #: $P < 0.05$, compared with the HSPS group; &: $P < 0.05$, compared with the HSPS-VEGF group; \$: $P < 0.05$, compared with the HSPS-SC group.

autograft and the HSPS-SC (VEGF) group (Fig. 8A). Black polyaniline (PANI) particles were found to be distributed in nerve of all conduit groups, which indicated that the HSPS conduits were dispersed along with the nerve regeneration.

CD31, also known as PECAM-1, is the key biomarkers of blood vessels. The CD31 IHC-staining images are shown in Fig. 8B. The CD31⁺ stained cells of HSPS-SC and Autograft groups was more than that of HSPS, HSPS-VEGF and HSPS-SC groups. CD34 is a transmembrane protein marker in the vascular tissues [34], α -SMA is the important biomarker of parietal cells in newborn blood vessels [35]. According to the CD34/ α -SMA co-immunofluorescence results (Fig. 8C), the neovascularization density of each group was calculated. The neovascularization density of HSPS-SC group was higher than that of HSPS and HSPS-VEGF, while the neovascularization density of HSPS-SC (VEGF) and autograft groups was higher than that of HSPS, HSPS-VEGF and HSPS-SC groups (Fig. 8D).

In order to quantitatively analyze the relative expression levels of CD31 in each group, Western blot analysis was also performed using regenerated nerves (Fig. 8E). There was no difference in CD31 expression levels between autograft and HSPS-SC (VEGF), while CD31 expression levels in HSPS, HSPS-VEGF and HSPS-SC groups were lower than those in autograft and HSPS-SC (VEGF) groups. Besides, the expression levels of CD31 in HSPS-SC was higher than those in HSPS and HSPS-VEGF groups.

According to H&E-staining, CD31 IHC-staining, CD34/ α -SMA IF-staining and Western Blot analysis, exogenous VEGF-A cannot effectively promote angiogenesis during nerve regeneration process because it may drift away from the HSPS conduit, while Schwann cells over-expressing VEGF-A could significantly improve the angiogenesis via slow release of VEGF-A.

3.9. Possible molecular mechanism of angiogenesis

The possible molecular mechanism for the improved angiogenesis in HSPS-SC(VEGF) group were further explored. Total proteins were extracted from the regenerated nerve for Western blot analysis (Fig. 9). There was no significant difference in VEGFR2 and ERK expression levels among the five experiment groups. However, there were significant differences of phosphorylated VEGFR2 and ERK proteins among the five groups. p-VEGFR2/VEGFR2 relative expression levels were significantly lower in the four conduit groups than in the Autograft group. The p-VEGFR2/VEGFR2 relative expression levels in HSPS-SC(VEGF) group was higher than those in HSPS, HSPS-VEGF and HSPS-SC groups, while those in HSPS-SC group were dramatically higher than those in HSPS and HSPS-VEGF groups. Meanwhile, the p-ERK/ERK relative expression levels in autograft and HSPS-SC(VEGF) were the highest among the five groups, and there was no difference between them. The relative expression levels of p-ERK/ERK were dramatically elevated in the HSPS-SC group comparing to those in the HSPS and HSPS-VEGF groups.

These data together revealed that Schwann cells could efficiently promote the activation of VEGF/VEGFR2/ERK signaling pathway. VEGF-A overexpressed by Schwann cells could elevate the activation of VEGF/VEGFR2/ERK signaling even greater, which may contribute to the accelerated angiogenesis in the corresponding groups in sciatic nerve repair.

4. Discussion

In our previous work, the cell viability and cell contact experiments of HSPS, and systemic toxicity assessment all proved the good biocompatibility of HSPS [27,28]. In this research, a comprehensive strategy for peripheral nerve repair is put forward by combination of the flexible HSPS conduits, Schwann cells as seed cells, and VEGF-A. Most of the

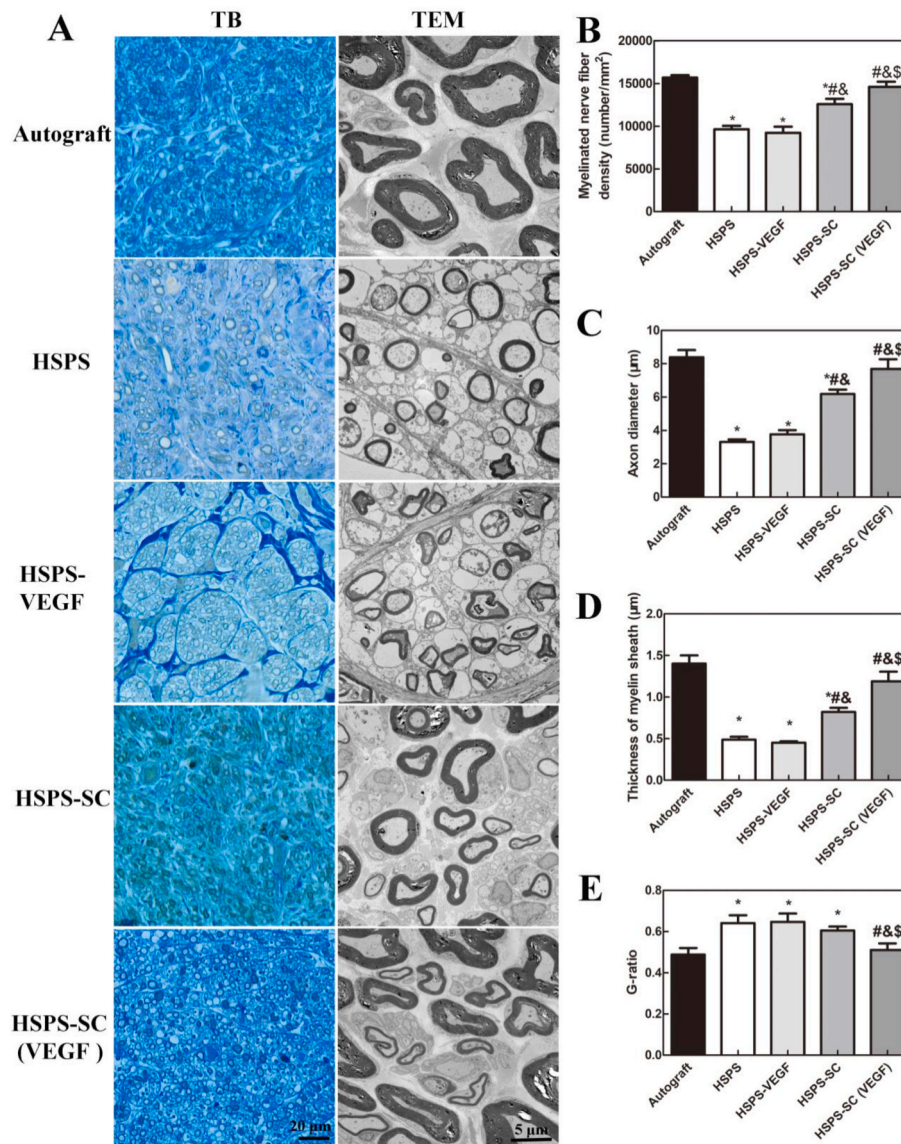


Fig. 6. Myelinated nerve analysis of regenerated nerve. (A) Toluidine blue (TB) staining and TEM images of regenerated nerves; (B, C, D and E) Analysis of the myelinated nerve fibers based on toluidine blue staining and TEM images, n = 5, *: $P < 0.05$, compared with the Autograft group; #: $P < 0.05$, compared with the HSPS group; &: $P < 0.05$, compared with the HSPS-VEGF group; \$: $P < 0.05$, compared with the HSPS-SC group.

parameters of nerve regeneration in the HSPS-SC (VEGF) group showed no difference from those in the autograft group, except the electrophysiological result. In our previous study, cellulose/SPI conduits combined with Schwann cells could support some extent nerve regeneration, but it still far from the recovery efficiency of the autograft group [12]. Moreover, chitosan conduits containing engineered Schwann cells overexpressing GDNF could not effectively promote nerve regeneration [16]. Altogether, the choice of conduit, seed cells and factors and the combination could be critical to meet the high requirements of nerve regeneration. Angiogenesis, myelin regeneration and axon regeneration occur in sequence in the process of nerve regeneration, and the angiogenesis is the initial and crucial stage for nerve regeneration. VEGF-A is the key growth factor in angiogenesis, and Schwann cells themselves can secrete VEGF-A which may be not sufficient to effectively promote angiogenesis. Therefore, the strategy in our study followed the process of the nerve regeneration, which could dramatically elevate the efficiency of nerve repair.

Schwann cells transfected with control lentivirus adhered to the HSPS nerve guide conduits (HSPS-SC group), were used as one of the control groups. The results of SFI, electrophysiology, gastronomic

muscle recovery, toluidine blue staining, TEM, NF200/S100 staining and angiogenesis effect were lower in the HSPS-SC group than those in the HSPS-SC (VEGF) group. These data indicate that VEGF-A has excellent effects on nerve repair, since VEGF-A is reported one of the most potential growth factors to promote the formation of new blood vessels [36]. It is reported that BMSCs-transfected VEGF could significantly improve vascularization and osteogenesis for *in vivo* bone healing [37]. Moreover, the intramuscular gene transfer of VEGF encoding plasmid enhances motor and sensory functions in a rabbit model of ischemic peripheral neuropathy [38].

Schwann cells are the primary inducers of regeneration in the peripheral nervous system. Schwann cells can be isolated from adult peripheral nerves, expanded in large numbers, and genetically transduced by viral vectors *in vitro* prior to their use *in vivo* [24]. VEGF-A is a key component of successful blood vessels and nerves regeneration [18]. Therefore, VEGF-overexpressing-Schwann cell loaded HSPS showed a good potential for clinical application. As many literatures reported that lentivirus-infected hematopoietic stem cells showed excellent therapeutic effect and good safety performance for clinical therapy [26,39]. Moreover, lots of strategies are developed to mitigate the risks of using

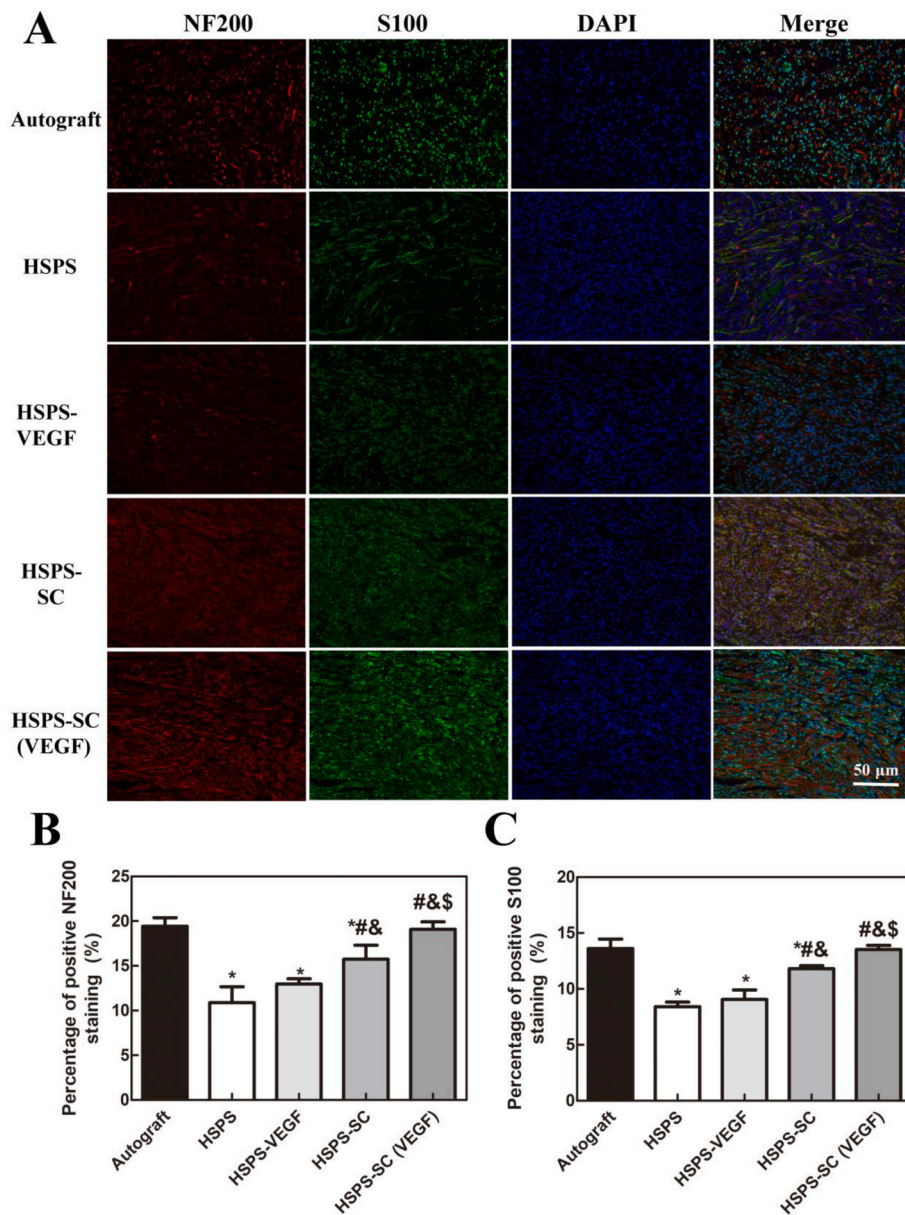


Fig. 7. Immunofluorescence analysis of the regenerated nerves. (A) Images of NF200 and S100 immunofluorescence staining; The statistical results of percentage of positive NF200 staining (B) and percentage of positive S100 staining (C), n = 5, *: P < 0.05, compared with Autograft; #: P < 0.05, compared with the HSPS group; &: P < 0.05, compared with the HSPS-VEGF group; \$: P < 0.05, compared with the HSPS-SC group.

lentivirus plasmid in medical therapy [26].

The GFP-labeled Schwann cells could be detected at 3 months after transplantation, which demonstrated the *in vivo* activity of allogeneic Schwann cells. This is supported by the report that GFP-labeled Schwann cells could survive after 16 weeks' transplantation [24]. The immunofluorescent co-staining of GFP/VEGF-A, Ki67 and MBP showed that the VEGF-A overexpressing Schwann cells could promote the proliferation, migration and differentiation of Schwann cells as the VEGF-A was secreted from the VEGF-A overexpressing Schwann cells. This is consistent with the report that VEGF-A can promote the proliferation, migration and differentiation of Schwann cells through the endocrine loop [21].

Our data together with these reports revealed that the deliver method of VEGF is also critical to enhance the nerve repairing efficiency. The routine strategies for depositing nerve growth factors in nerve tissue engineering scaffolds include physical adsorption and the chemical covalent binding. The posterior physical strategies are more stable in

accomplishing predictive drug release. But they involve complicated procedures during scaffold fabrication which may compromise protein bioactivity and receptor binding ability [40]. It is a simple and direct method to adsorb the growth factor in the as-prepared scaffolds. Hence, the flexible and porous HSPS conduits adsorbing VEGF-A growth factor were worked as a control group (HSPS-VEGF group) in our study. At the same time, HSPS-SC(VEGF) conduits may provide sustained delivery of VEGF-A during the nerve regeneration process as endogenous secretion group. The angiogenesis, SFI, electrophysiology, gastronomic muscle recovery, toluidine blue staining, TEM and NF200/S100 staining was much better in the HSPS-SC(VEGF) group (endogenous secretion group) than that in the HSPS-VEGF group (exogenous secretion group).

These aspects may cause the failure of accelerating angiogenesis in HSPS-VEGF group: The exogenous VEGF-A growth factor absorbed by the porous HSPS scaffolds suffers from a short half-life and the VEGF-A growth factor may be sensitive to the *in vivo* microenvironment; The quick release of VEGF-A (in two days) have side effects such as

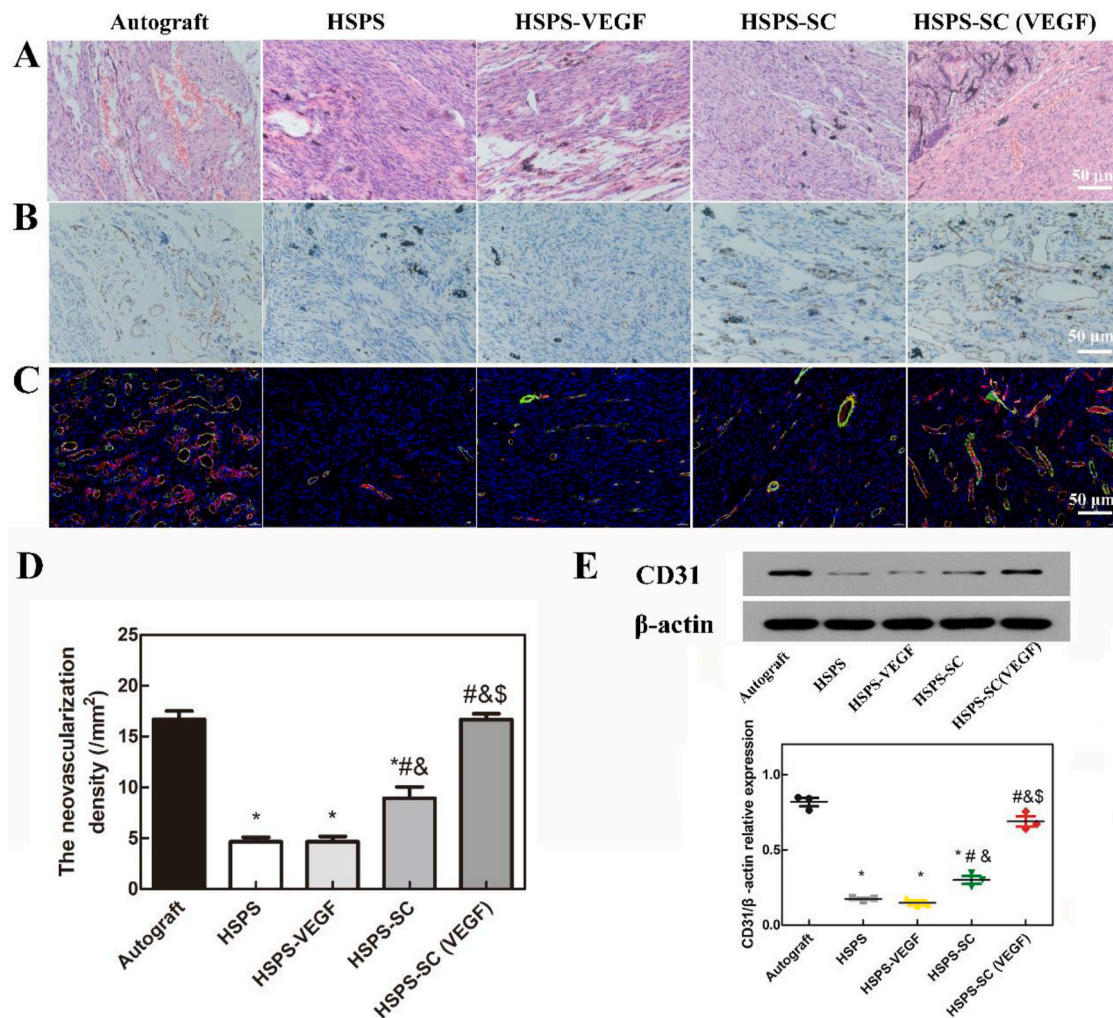


Fig. 8. Evaluation of angiogenesis. (A) Images of HE-stained longitudinal sections of the regenerated nerve; Images of CD31 IHC-stained (B) and CD34 (green)/ α -SMA (red) IF-stained (C) Longitudinal sections of the regenerated nerve; (D) The neovascularization density of the regenerated nerve, $n = 5$; (E) Western blot analysis of CD31 proteins expression of the regenerated nerve, $n = 3$, *, $P < 0.05$, compared with the Autograft group; #: $P < 0.05$, compared with the HSPS group; &: $P < 0.05$, compared with the HSPS-VEGF group; \$: $P < 0.05$, compared with the HSPS-SC group.

vasodilation and inadequate vascularization [41]. Unlike exogenous VEGF-A groups, the engineered Schwann cells in HSPS-SC (VEGF) group could secrete many nerve factors besides VEGF, such as gliotrophic and neurotrophic factors. These growth factors may perform many functions: protecting the survive of motor and sensory neurons, and stimulating the neurons or glia cells to proliferate and migrate in an autocrine loop model [21]. On the other hand, VEGF-A secreted by the Schwann cells loaded in HSPS-SC(VEGF) conduits could bind to VEGF receptor (VEGFR2) to induce proliferation, adhesion and migration of both vascular endothelial cells and Schwann cells, thereby enhancing the activation of downstream angiogenic signaling pathway [42].

In our study, no significant difference of VEGFR2 protein expression was shown among the five groups, while the expression levels of p-VEGFR2 in HSPS-SC(VEGF) group was significantly higher than that in the HSPS-VEGF group, implying that VEGF-A proteins secreted by Schwann cells were bioactive and promoted the phosphorylation of VEGFR2 protein. ERK is a downstream molecule regulated by VEGF signaling cascades [43], and the activation of ERK in the HSPS-SC (VEGF) group is prominently higher than that in HSPS-VEGF group, suggesting that VEGF-A mediated activation of VEGFR2 may contribute to the enhanced intracellular ERK protein activation. Together with the significant regulatory effect of HSPS-SC(VEGF) conduits on angiogenesis, it was speculated that the HSPS-SC (VEGF) nerve conduits may

regulate the angiogenesis during nerve regeneration via the VEGFR2/ERK signaling pathway. The above mechanism is one potential pro-angiogenic molecular mechanism in nerve regeneration. In the future research, more efforts will be taken to identify critical molecular mechanisms that control angiogenesis, which is of great significance for peripheral nerve regeneration.

5. Conclusions

The VEGF-A overexpressing Schwann cells could be combined with HSPS conduits for efficient sciatic nerve repair. The VEGF-A overexpressing Schwann cells had improved proliferation, migration and differentiation ability. Effects of HSPS-SC(VEGF) conduits on nerve regeneration were assessed *in vivo*, and the results showed excellent functional and morphological recovery. This may elevate angiogenesis and then promote the nerve regeneration by synergistic effects of VEGF-A and Schwann cells. The possible molecular mechanism might be related to elevated activation of the VEGFR2/ERK signaling pathway. Therefore, the Schwann cells mediated, VEGF-A modified microenvironment and HSPS conduit guided nerve regeneration provide an excellent comprehensive strategy of peripheral nerve regeneration, which may afford a new avenue to enhance proangiogenic and nerve regeneration capacity in nerve injury repair.

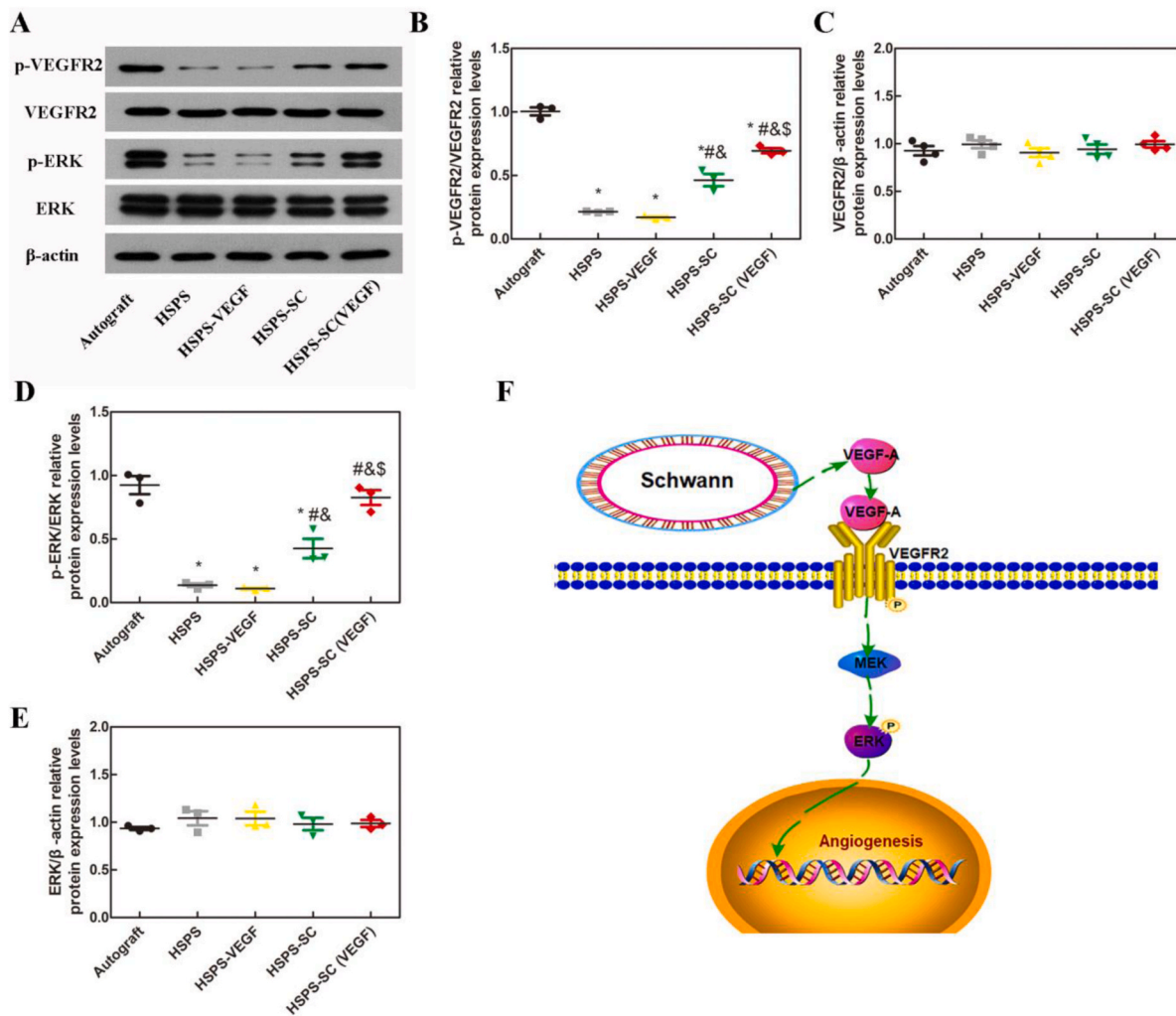


Fig. 9. Western Blot analysis. (A) Western Blot of the regenerated nerve in each group; (B) Western Blot analysis of p-VEGFR2/VEGFR2 proteins expression; (C) Western Blot analysis of VEGFR2/β-actin proteins expression; (D) Western Blot analysis of p-ERK/ERK proteins expression; (E) Western Blot analysis of ERK/β-actin proteins expression; (F) Possible mechanisms of VEGF-A overexpressing Schwann cells to nerve regeneration, n = 3, *: P < 0.05, compared with the Autograft group; #: P < 0.05, compared with the HSPS group; &: P < 0.05, compared with the HSPS-VEGF group; \$: P < 0.05, compared with the HSPS-SC group.

Declaration of competing InterestCOI

The authors declare no competing financial interest.

CRedit authorship contribution statement

Ping Wu: Formal analysis, Writing – original draft. **Zan Tong:** Formal analysis, Writing – original draft, Writing – review & editing. **Lihua Luo:** Writing – review & editing. **Yanan Zhao:** Methodology. **Feixiang Chen:** Methodology. **Yinping Li:** Methodology. **Céline Huselstein:** Writing – review & editing. **Qifa Ye:** Supervision. **Qingsong Ye:** Supervision, Funding acquisition. **Yun Chen:** Conceptualization, Funding acquisition, Supervision.

Acknowledgments

This work was supported by the National Natural Science Foundation of China (Grant No.: NSFC 81871493, 81871503), and the Medical Science Advancement Program (Clinical Medicine) of Wuhan University (Grant No.: TFLC2018002, 2018003). Thanks for the technique support from the Experimental Teaching Center of Basic Medical Sciences, Wuhan University.

Appendix A. Supplementary data

Supplementary data to this article can be found online at <https://doi.org/10.1016/j.bioactmat.2021.03.020>.

References

- [1] M.D. Sarker, N. Saman, A.D. McInnes, D.J. Schreyer, C. Xiongbiao, Regeneration of peripheral nerves by nerve guidance conduits: influence of design, biopolymers, cells, growth factors, and physical stimuli, *Prog. Neurobiol.* 171 (2018) 125–150, <https://doi.org/10.1016/j.pneurobio.2018.07.002>.
- [2] K. Zhang, W.H. Chooi, S. Liu, J.S. Chin, A. Murray, D. Nizetic, D. Cheng, S.Y. Chew, Localized delivery of CRISPR/dCas9 via layer-by-layer self-assembling peptide coating on nanofibers for neural tissue engineering, *Biomaterials* 256 (2020) 120225, <https://doi.org/10.1016/j.biomaterials.2020.120225>.
- [3] L. Zhang, W. Yang, H. Xie, H. Wang, J. Wang, Q. Su, X. Li, Y. Song, G. Wang, L. Wang, Z. Wang, Sericin nerve guidance conduit delivering therapeutically repurposed clobetasol for functional and structural regeneration of transected peripheral nerves, *ACS Biomater. Sci. Eng.* 5 (2019) 1426–1439, <https://doi.org/10.1021/acsbomaterials.8b01297>.
- [4] L. He, Z. Sun, J. Li, R. Zhu, B. Niu, K.L. Tam, Q. Xiao, J. Li, W. Wang, C.Y. Tsui, W. Hong Lee, K.F. So, Y. Xu, S. Ramakrishna, Q. Zhou, K. Chiu, Electrical stimulation at nanoscale topography boosts neural stem cell neurogenesis through the enhancement of autophagy signaling, *Biomaterials* 268 (2021) 120585, <https://doi.org/10.1016/j.biomaterials.2020.120585>.
- [5] Q. Qian, H.Y. Meng, B. Chang, G.B. Liu, X.Q. Cheng, H. Tang, Y. Wang, J. Peng, Q. Zhao, S.B. Lu, Aligned fibers enhance nerve guide conduits when bridging

- peripheral nerve defects focused on early repair stage, *Neural Regen Res* 14 (2019) 903–912, <https://doi.org/10.4103/1673-5374.249239>.
- [6] S. Vijayavenkataraman, S. Thaharah, S. Zhang, W.F. Lu, J.Y.H. Fuh, Electrohydrodynamic jet 3D-printed PCL/PAA conductive scaffolds with tunable biodegradability as nerve guide conduits (NGCs) for peripheral nerve injury repair, *Mater. Des.* 162 (2019) 171–184, <https://doi.org/10.1016/j.matdes.2018.11.044>.
- [7] M. Salehi, Z. Bagher, S.K. Kamrava, A. Ehterami, R. Alizadeh, M. Farhadi, M. Falah, A. Komeili, Alginate/chitosan hydrogel containing olfactory ectomesenchymal stem cells for sciatic nerve tissue engineering, *J. Cell. Physiol.* 234 (2019) 15357–15368, <https://doi.org/10.1002/jcp.28183>.
- [8] L. Luo, Y. He, L. Jin, Y. Zhang, F.P. Guastaldi, A.A. Albashari, F. Hu, X. Wang, L. Wang, J. Xiao, L. Li, J. Wang, A. Higuchi, Q. Ye, Application of bioactive hydrogels combined with dental pulp stem cells for the repair of large gap peripheral nerve injuries, *Bioact Mater* 6 (2021) 638–654, <https://doi.org/10.1016/j.bioactmat.2020.08.028>.
- [9] C.F. Su, L.H. Chang, C.Y. Kao, D.C. Lee, K.H. Cho, L.W. Kuo, H. Chang, Y.H. Wang, I.M. Chiu, Application of amniotic fluid stem cells in repairing sciatic nerve injury in minipigs, *Brain Res.* 1678 (2018) 397–406, <https://doi.org/10.1016/j.brainres.2017.11.010>.
- [10] H. Xu, Y. Yan, S. Li, PDLLA/chondroitin sulfate/chitosan/NGF conduits for peripheral nerve regeneration, *Biomaterials* 32 (2011) 4506–4516, <https://doi.org/10.1016/j.biomaterials.2011.02.023>.
- [11] L. Luo, W. Gong, Y. Zhou, L. Yang, D. Li, C. Huselstein, X. Wang, X. He, Y. Li, Y. Chen, Cellulose/soy protein isolate composite membranes: evaluations of in vitro cytocompatibility with Schwann cells and in vivo toxicity to animals, *Bio Med. Mater. Eng.* 25 (2015) 57–64, <https://doi.org/10.3233/BME-141228>.
- [12] L. Luo, L. Gan, Y. Liu, W. Tian, Z. Tong, X. Wang, C. Huselstein, Y. Chen, Construction of nerve guide conduits from cellulose/soy protein composite membranes combined with Schwann cells and pyrroloquinoline quinone for the repair of peripheral nerve defect, *Biochem. Biophys. Res. Commun.* 457 (2015) 507–513, <https://doi.org/10.1016/j.bbrc.2014.12.121>.
- [13] F. Gonzalez-Perez, J. Hernandez, C. Heimann, J.B. Phillips, E. Udina, X. Navarro, Schwann cells and mesenchymal stem cells in laminin- or fibronectin-aligned matrices and regeneration across a critical size defect of 15 mm in the rat sciatic nerve, *J. Neurosurg. Spine* 28 (2018) 109–118, <https://doi.org/10.3171/2017.5.SPINE161100>.
- [14] A. Resch, S. Wolf, A. Mann, T. Weiss, A.L. Stetco, C. Radtke, Co-culturing human adipose derived stem cells and Schwann cells on spider silk-A new approach as prerequisite for enhanced nerve regeneration, *Int. J. Mol. Sci.* 20 (2018) 1–11, <https://doi.org/10.3390/ijms20010071>.
- [15] S. Vijayavenkataraman, Nerve guide conduits for peripheral nerve injury repair: a review on design, materials and fabrication methods, *Acta Biomater.* 106 (2020) 54–69, <https://doi.org/10.1016/j.actbio.2020.02.003>.
- [16] C. Meyer, S. Wrobel, S. Raimondo, S. Rochkind, C. Heimann, A. Shahar, O. Ziv-Polat, S. Geuna, C. Grothe, K. Haastert-Talini, Peripheral nerve regeneration through hydrogel-enriched chitosan conduits containing engineered Schwann cells for drug delivery, *Cell Transplant.* 25 (2016) 159–182, <https://doi.org/10.3727/096368915X688010>.
- [17] B. Hou, Z. Ye, W. Ji, M. Cai, C. Ling, C. Chen, Y. Guo, Comparison of the effects of BMSC-derived Schwann cells and autologous Schwann cells on remyelination using a rat sciatic nerve defect model, *Int. J. Biol. Sci.* 14 (2018) 1910–1922, <https://doi.org/10.7150/ijbs.26765>.
- [18] A.L. Cattin, J.J. Burden, L. Van Emmenis, F.E. Mackenzie, J.J. Hoving, N. Garcia Calavia, Y. Guo, M. McLaughlin, L.H. Rosenberg, V. Quereda, D. Jacezna, I. Napoli, S. Parrinello, T. Enver, C. Ruhrberg, A.C. Lloyd, Macrophage-Induced blood vessels guide Schwann cell-mediated regeneration of peripheral nerves, *Cell* 162 (2015) 1127–1139, <https://doi.org/10.1016/j.cell.2015.07.021>.
- [19] Y.Z. Kunlin, Jin Yunjuan, Sun Xiao, Ou Mao, Lin Xie, David A. Greenberg, Vascular endothelial growth factor (VEGF) stimulates neurogenesis in vitro and in vivo, *Proc. Natl. Acad. Sci. Unit. States Am.* 99 (2002) 11946–11950, <https://doi.org/10.1073/pnas.182296499>.
- [20] N. Mokarram, A. Merchant, V. Mukhatyar, G. Patel, R.V. Bellamkonda, Effect of modulating macrophage phenotype on peripheral nerve repair, *Biomaterials* 33 (2012) 8793–8801, <https://doi.org/10.1016/j.biomaterials.2012.08.050>.
- [21] Jeffrey M. Rosenstein, Janette M. Krum, Christiana Ruhrberg, VEGF in the nervous system, *Organogenesis* 6 (2010) 107–114, <https://doi.org/10.4161/org.6.2.11687>.
- [22] X. Tang, H. Qin, X. Gu, X. Fu, China's landscape in regenerative medicine, *Biomaterials* 124 (2017) 78–94, <https://doi.org/10.1016/j.biomaterials.2017.01.044>.
- [23] K.A. Langert, E.M. Brey, Strategies for targeted delivery to the peripheral nerve, *Front. Neurosci.* 12 (2018) 887, <https://doi.org/10.3389/fnins.2018.00887>.
- [24] A.V. Berrocal Ya, R. Gupta, A.D. Levi, Transplantation of Schwann cells in a collagen tube for the repair of large, segmental peripheral nerve defects in rats, *J. Neurosurg.* 119 (2013) 720–732, <https://doi.org/10.3171/2013.4.JNS121189>.
- [25] C.O. Goulart, S. Jurgensen, A. Souto, J.T. Oliveira, S. de Lima, C. Tonda-Turo, S. A. Marques, F.M. de Almeida, A.M. Martinez, A combination of Schwann-cell grafts and aerobic exercise enhances sciatic nerve regeneration, *PLoS One* 9 (10) (2014), e110090, <https://doi.org/10.1371/journal.pone.0110090>.
- [26] X.M. Anguela, K.A. High, Entering the modern era of gene therapy, *Annu. Rev. Med.* 70 (2019) 273–288, <https://doi.org/10.1146/annurev-med-012017-043332>.
- [27] P. Wu, A. Xiao, Y. Zhao, F. Chen, M. Ke, Q. Zhang, J. Zhang, X. Shi, X. He, Y. Chen, An implantable and versatile piezoresistive sensor for the monitoring of human-machine interface interactions and the dynamical process of nerve repair, *Nanoscale* 11 (2019) 21103–21108, <https://doi.org/10.1039/c9nr03925b>.
- [28] P. Wu, Y. Zhao, F. Chen, A. Xiao, Q. Du, Q. Dong, M. Ke, X. Liang, Q. Zhou, Y. Chen, Conductive hydroxyethyl cellulose/soy protein isolate/polyaniline conduits for enhancing peripheral nerve regeneration via electrical stimulation, *Front. Bioeng. Biotechnol.* 8 (2020) 709, <https://doi.org/10.3389/fbioe.2020.00709>.
- [29] Y. Zhao, Q. Zhang, L. Zhao, L. Gan, L. Yi, Y. Zhao, J. Xue, L. Luo, Q. Du, R. Geng, Z. Sun, N. Benkirane-Jessel, P. Chen, Y. Li, Y. Chen, Enhanced peripheral nerve regeneration by a high surface area to volume ratio of nerve conduits fabricated from hydroxyethyl cellulose/soy protein composite sponges, *ACS Omega* 2 (2017) 7471–7481, <https://doi.org/10.1021/acsomega.7b01003>.
- [30] Y. Zhao, M. He, L. Zhao, S. Wang, Y. Li, L. Gan, M. Li, L. Xu, P.R. Chang, D. P. Anderson, Y. Chen, Epichlorohydrin-Cross-linked hydroxyethyl cellulose/soy protein isolate composite films as biocompatible and biodegradable implants for tissue engineering, *ACS Appl. Mater. Interfaces* 8 (2016) 2781–2795, <https://doi.org/10.1021/acsmi.5b11152>.
- [31] G.C. Hobson Mi, G. Terenghi, VEGF enhances intraneural angiogenesis and improves nerve regeneration after axotomy, *J. Anat.* 197 (2000) 591–605, <https://doi.org/10.1046/j.1469-7580.2000.19740591.x>.
- [32] G. Wang, W. Wu, H. Yang, P. Zhang, J.Y. Wang, Intact polyaniline coating as a conductive guidance is beneficial to repairing sciatic nerve injury, *J. Biomed. Mater. Res. B Appl. Biomater.* 108 (2019) 128–142, <https://doi.org/10.1002/jbm.b.34372>.
- [33] C.L. Liu Wang, Shuhui Yang, Pengcheng Sun, Yu Wang, Yanjun Guan, Shuang Liu, Dalí Cheng, Haoye Meng, Qiang Wang, Jianguo He, Hanqing Hou, Li Huo, Wei Lu, Yanxu Zhao, Jing Wang, Yaqiong Zhu, Yunxuan Li, Luo Dong, Li Tong, Hao Chen, Shirong Wang, Sheng Xing, Wei Xiong, Xiumei Wang, Peng Jiang, Lan Yin, A fully biodegradable and self-electrified device for neuroregenerative medicine, *Science Advances* 6 (2020), eabc6686, <https://doi.org/10.1126/sciadv.abc6686>.
- [34] Y. Cheng, Y. Xu, Y. Qian, X. Chen, Y. Ouyang, W.-E. Yuan, 3D structured self-powered PVDF/PCL scaffolds for peripheral nerve regeneration, *Nano Energy* 69 (2020) 104411, <https://doi.org/10.1016/j.nanoen.2019.104411>.
- [35] X. Zhang, G. Chen, Y. Liu, L. Sun, L. Sun, Y. Zhao, Black phosphorus-loaded separable microneedles as responsive oxygen delivery carriers for wound healing, *ACS Nano* 14 (2020) 5901–5908, <https://doi.org/10.1021/acsnano.0c01059>.
- [36] L.H. Solis, Y.M. Ayala-Marin, S. Portillo, A. Varela-Ramirez, R.J. Aguilera, T. Boland, Thermal inkjet bioprinting triggers the activation of the VEGF pathway in human microvascular endothelial cells in vitro, *Biofabrication* 11 (2019), 045005, <https://doi.org/10.1088/1758-5090/ab25f9>.
- [37] F. Geiger, H. Lorenz, W. Xu, K. Szalay, P. Kasten, L. Claes, P. Augat, W. Richter, VEGF producing bone marrow stromal cells (BMSC) enhance vascularization and resorption of a natural coral bone substitute, *Bone* 41 (2007) 516–522, <https://doi.org/10.1016/j.bone.2007.06.018>.
- [38] S.G. Schratzberger P, M. Silver, Favorable effect of VEGF gene transfer on ischemic peripheral neuropathy, *Nat. Med.* 6 (2000) 405–413, <https://doi.org/10.1038/74664>.
- [39] Nathalie Cartier, Salima Hacein-Bey-Abina, Cynthia C. Bartholomae, Gabor Veres, Manfred Schmidt, Ina Kutschera, Michel Vidaud, Ulrich Abel, Liliane Dal-Cortivo, Laure Caccavelli, Nizar Mahlaoui, Véronique Kiermer, Denice Mittelstaedt, Céline Bellesse, Najiba Lahlou, François Lefrère, Stéphane Blanche, Muriel Audit, Emmanuel Payen, Philippe Leboulch, Bruno l'Homme, Pierre Bougnères, Christof Von Kalle, Alain Fischer, Marina Cavazzana-Calvo, Patrick Aubourg, Hematopoietic stem cell gene therapy with a lentiviral vector in X-linked adrenoleukodystrophy, *Science* 326 (2009) 818–823, <https://doi.org/10.1126/science.1171242>.
- [40] S. Singh, B.M. Wu, J.C. Dunn, Delivery of VEGF using collagen-coated polycaprolactone scaffolds stimulates angiogenesis, *J. Biomed. Mater. Res.* 100 (2012) 720–727, <https://doi.org/10.1002/jbm.a.34010>.
- [41] P. Muangsant, R.J. Shipley, J.B. Phillips, Vascularization strategies for peripheral nerve tissue engineering, *Anat. Rec.* 301 (2018) 1657–1667, <https://doi.org/10.1002/ar.23919>.
- [42] J. Angulo, C. Peiro, T. Romacho, A. Fernandez, B. Cuevas, R. Gonzalez-Corrochano, G. Gimenez-Gallego, I.S. de Tejada, C.F. Sanchez-Ferrer, P. Cuevas, Inhibition of vascular endothelial growth factor (VEGF)-induced endothelial proliferation, arterial relaxation, vascular permeability and angiogenesis by dobesilate, *Eur. J. Pharmacol.* 667 (2011) 153–159, <https://doi.org/10.1016/j.ejphar.2011.06.015>.
- [43] P. Secchiero, A. Gonelli, E. Carnevale, D. Milani, A. Pandolfi, D. Zella, G. Zauli, TRAIL promotes the survival and proliferation of primary human vascular endothelial cells by activating the Akt and ERK pathways, *Circulation* 107 (2003) 2250–2256, <https://doi.org/10.1161/01.CIR.0000062702.60708.C4>.